



Chemically complex intermetallic alloys: A new frontier for innovative structural materials

T. Yang^{1,2,*}, B.X. Cao^{1,2}, T.L. Zhang^{1,2}, Y.L. Zhao³, W.H. Liu³, H.J. Kong^{2,4}, J.H. Luan¹, J.J. Kai^{1,4}, W. Kuo⁴, C.T. Liu^{1,2,*}

¹ Department of Materials Science and Engineering, City University of Hong Kong, Hong Kong, China

² Hong Kong Institute for Advanced Study, City University of Hong Kong, Hong Kong, China

³ School of Materials Science and Engineering, Harbin Institute of Technology (Shenzhen), Shenzhen 518055, China

⁴ Department of Mechanical Engineering, City University of Hong Kong, Hong Kong, China

Intermetallic materials are bestowed by diverse ordered superlattice structures together with many unusual properties. In particular, the advent of chemically complex intermetallic alloys (CCIMAs) has received considerable attention in recent years and offers a new paradigm to develop novel metallic materials for advanced structural applications. These newly emerged CCIMAs exhibit synergistic modulations of structural and chemical features, such as self-assembled long-range close-packed ordering, complex sublattice occupancy, and interfacial disordered nanoscale layer, potentially allowing for superb physical and mechanical properties that are unmatched in conventional metallic materials. In this paper, we critically review the historical developments and recent advances in ordered intermetallic materials from the simple binary to chemically complex alloy systems. We are focused on the unique multicomponent superlattice microstructures, nanoscale grain-boundary segregation, and disordering, as well as the various extraordinary mechanical and functional properties of these newly developed CCIMAs. Finally, perspectives on the future research orientation, challenges, and opportunities of this new frontier are provided.

Keywords: Ordered superlattice; Intermetallic materials; Chemically complex alloys; Sublattice occupancy; Grain-boundary engineering

Introduction

Metallic materials can be roughly divided into two major categories: one with disordered atomic structures and the other with ordered atomic structures. As a unique type of alloys, intermetallic materials with ordered superlattice structures have drawn tremendous attention in a broad range of modern industries due to their many unique structures and properties, including long-range ordering, strong atomic bonding, site-isolation effect, high strength, high melting points, good corrosion, and oxidation resistance, etc. [1–15]. For example, many ordered intermetallic phases or alloys possess stable long-range ordered

crystalline structures even up to their melting points [2,7,10]. Stronger binding and closer packing between various atomic species enable them to have restricted atomic mobility and sluggish lattice diffusion, as well as better resistance to creep [1,4]. More importantly, these alloys generally exhibit the unusual yield stress anomaly behaviors, namely the increased rather than decreased yield strength with the increase of temperatures (see Fig. 1) [4,16–18]. All of these intriguing behaviors make them with a great prospect as high-temperature structural materials, which are crucial for a variety of important applications including aerospace, nuclear power, and chemical processing, etc.

However, ordered intermetallic alloys are generally susceptible to limited ductility and brittle fracture at ambient temperatures, which seriously limits their practical usability.

* Corresponding authors.

E-mail addresses: Yang, T. (taoyang6-c@my.cityu.edu.hk), Liu, C.T. (chainliu@cityu.edu.hk).

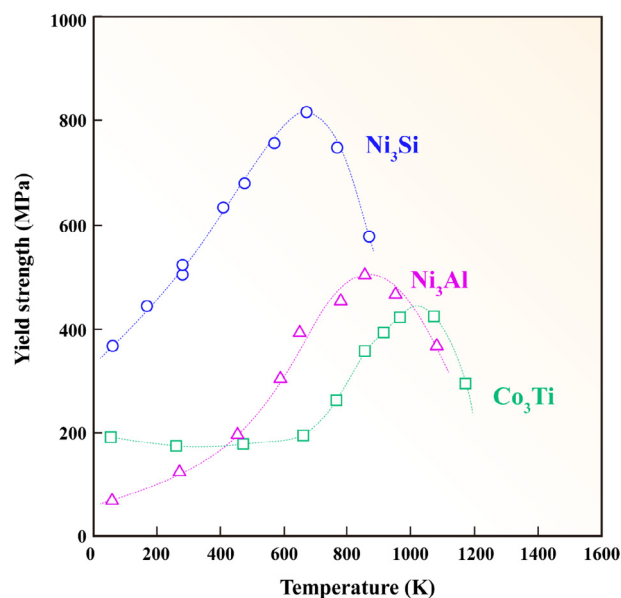


FIGURE 1

Yield strength anomaly behaviors observed in several binary intermetallic alloys with the L_{12} -type crystalline structure [18].

The embrittlement problem can be mainly caused by an insufficient number of slip systems (bulk brittleness) and poor grain boundary cohesion [5,19,20]. To overcome this thorny problem, during the past years, we have systematically investigated the physical metallurgy principles and mechanical behaviors of ordered intermetallic alloys, especially for the cubic ordered intermetallic alloys [5,10,14,21–25]. Various kinds of alloying processes (both macro-alloying and micro-alloying) and microstructural control techniques have been developed to intrinsically enhance their plastic deformation capacities [22–24]. For example, in the Ni_3V – Co_3V – Fe_3V alloy systems, tailoring the value of electron concentration (e/a) provides a very effective method to design the ductile ordered intermetallic alloys. By adding the Fe element, the brittle $(Ni,Co)_3V$ alloy can be significantly ductilized, as long as the valence electron concentration falls below about 7.85 [4,5]. Moreover, the tensile ductility of polycrystalline Ni_3Al alloys can be improved to some extent by micro-alloying of B, Zr, and Hf elements, which segregates to grain boundaries and helps to eliminate the easy crack propagation along with them [14].

Although many remarkable achievements have been obtained in the metallurgical design of structural intermetallic alloys, there still has a relentless quest to achieve significantly enhanced mechanical properties. However, the research mainstream in previous studies was mainly limited to the chemically simple systems, such as the Ni_3Al , Ni_3Si , $NiAl$, and $TiAl$ -based alloys, which in general only contains small amounts of other kinds of additional elements, leading to a seriously limited compositional space for further performance optimization. Recently, a new design concept of the CCIMAs (sometimes also referred to as multicomponent intermetallic alloys or high-entropy intermetallic alloys) has emerged that offers a new opportunity to overcome this dilemma. By uniquely combining the long-range ordered superlattice structures and concentrated alloying of multiple elements together with unusual synergistic effects, the

newly developed CCIMAs create a new frontier for innovative structural materials with potentially extraordinary mechanical and physical properties, e.g., superb strength-ductility combination at room temperature, excellent thermal stability, unique super-elasticity, and superior creep resistance [13,26–29].

To foster a greater interest in this field and accelerate its development, here we provide an overview of the recent important discoveries and advances in the development of CCIMAs. In particular, the CCIMAs with the cubic ordered structures will be highlighted here due to their great potential towards superior strength-ductility combination. We aim at focusing on some key fundamental issues related to this emerging field, including the unique ordered superlattice structure, grain-boundary segregation and phase transformation, atomic-scale microstructural characterization using state-of-the-art multi-scale analytical tools, as well as the various intriguing properties. Finally, challenges and prospects for the future development of this new class of CCIMAs are briefly highlighted.

On the concept of chemically complex intermetallic alloys (CCIMAs)

It is well known that the development of structural alloys was mostly based on the single-principal-element metallic systems, which, however, is increasingly difficult to meet the growing requirements of designing advanced modern alloys due to the quite limited freedom for compositional and microstructural adjustments. Similar to the design of common engineering materials (like steels), the development of structural intermetallic alloys was generally restricted within the chemically simple systems, such as the L_{12} -type A_3B alloy, with only one principal element occupying each specific sublattice [14,30]. Kolli et al. carefully analyzed over 4000 intermetallic compounds and summarized the top 20 most common parent (basic) crystal structures for the binary metallic alloys [31]. As presented in Fig. 2, the body-centered cubic (BCC) and face-centered cubic (FCC) parent crystal structures have the largest number of chemical orderings, primarily dominated by the B2 and L_{12} -type superlattice structures, respectively (see Fig. 2b) [31]. In comparison with the low-symmetry crystalline structures (such as ordered hexagonal structure, topologically close-packed structure), the high-symmetry B2 and L_{12} superlattices with cubic ordered structures inherently have adequate independent slip systems, which allow for achieving decent plastic deformation capabilities in principle [5,32]. This intriguing fact has attracted significant research interests during past decades to develop structural intermetallic materials. Nevertheless, research on the chemically simple intermetallic systems has encountered a bottleneck, and the mechanical properties achieved previously are still unsatisfactory so far.

Recently, the metallurgical design by multicomponent alloying in multi-principal-element systems has been proposed, which offers a promising pathway for designing novel metallic materials with optimal properties [33–37]. To further improve the comprehensive performance of the intermetallic alloys, the design trend has been shifted to the chemically complex systems, radically departing from conventional compositional regions [13,28,38–45]. For example, motivated by the ductile multicomponent intermetallic nanoparticles formed in the

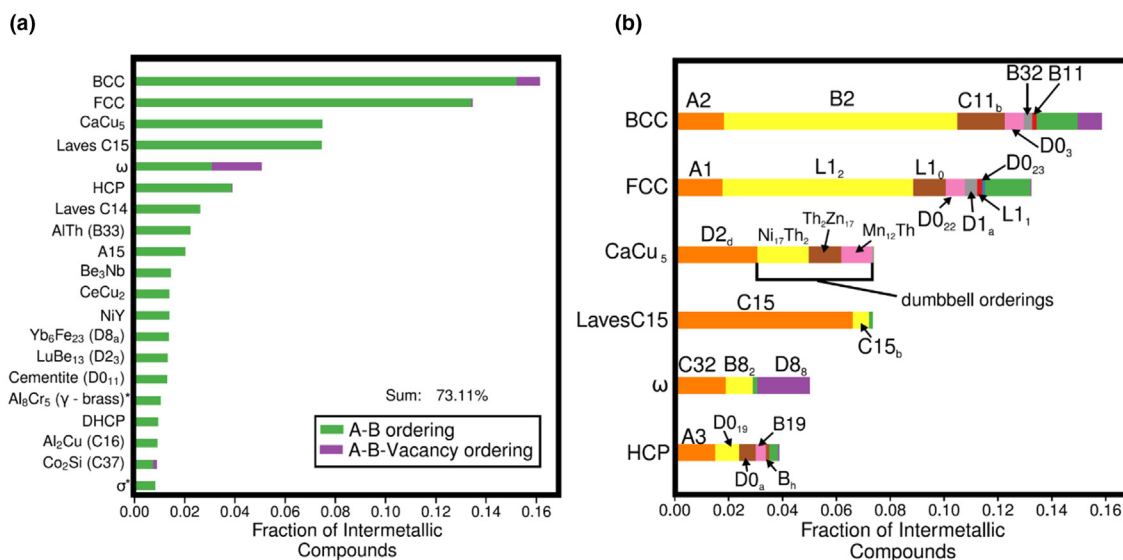


FIGURE 2

(a) The distribution of intermetallic compounds across the top 20 most common parent crystal structures for binary metallic alloys [31]. (b) The breakdown of ordered intermetallic compounds among the top six most common parent crystal structures for binary metallic alloys in (a). Ordering with specific Strukturbericht prototype structures are labeled. The green blocks represent orderings that do not have a Strukturbericht prototype name. The purple blocks represent orderings that contain vacancies. [31].

precipitation-hardened high-entropy alloys [33], Yang et al. fabricated the bulk $(\text{Ni}, \text{Co}, \text{Fe})_3(\text{Al}, \text{Ti}, \text{Fe})$ -type CCIMAs with a highly alloyed $L1_2$ -type structure, which was demonstrated with outstanding mechanical properties and thermal stability [13]. It was revealed that the Ti and Al atoms mainly occupy the vertices of the $L1_2$ unit cell, whereas the faced-centered positions are mainly occupied by Ni and Co atoms. It is interesting to find that the Fe atoms can occupy both the sublattice sites for maintaining the alloy stoichiometry. Although it has the $L1_2$ crystalline structure, such an atypical superlattice of the $(\text{Ni}, \text{Co}, \text{Fe})_3(\text{Al}, \text{Ti}, \text{Fe})$ -type structure is completely different from its binary Ni_3Al counterpart. Such a distinctly different site-occupation behavior are expected to bring about unique electronic structures, energy states, deformation substructures, and final properties of these alloys. Moreover, Zhou et al. synthesized several single-phase CCIMAs with a B2-type ordered structure, e.g., the $(\text{Fe}_{1/5}\text{Co}_{1/5}\text{Ni}_{1/5}\text{Mn}_{1/5}\text{Cu}_{1/5})\text{Al}$ alloy [39]. Five transition metal elements, e.g., Fe, Co, Ni, Mn, and Cu of equimolar fractions, occupy one sublattice, with Al on the other sublattice. More recently, Feng et al. discovered a novel ductile-transformable multicomponent B2-type intermetallic phase with a composition of $\text{Ni}_{32.3}\text{Fe}_{12.1}\text{Cr}_{8.8}\text{Co}_{16.9}\text{Al}_{29.9}$ (at.%) in a fatigue-resistant high-entropy alloys. Distinct from the traditional B2-type intermetallic phase that cannot bear too much plasticity in large sizes, it was found that these quinary B2 phases can deform plastically without microcracking during tensile deformation, suggesting the intrinsic ductile nature of this kind of chemically complex B2 intermetallic phase [46]. A direct comparison between the simple binary and chemically complex $L1_2$ and B2-type superlattice structures was illustrated schematically in Fig. 3. In view of the chemically complex site occupancy, a unique “sublattice high-entropy effect” with distinctive physical and/or chemical synergism can be expected, which would produce great impacts on the electronic structures, energy states, deformation substructures, and final

properties of these alloys. More importantly, the grain-boundary structures could also be significantly altered due to the complex alloying of multiple elements [13,44]. In brief, the concept of CCIMAs provides a new and promising research direction for designing ordered intermetallic alloys with a vast range of possibilities.

Unique microstructures of CCIMAs

In this section, we would like to summarize the milestone progress in the development of CCIMAs, including the control of ordered crystal structures, engineering of grain-boundary chemistries and structures. Additionally, the multiscale characterizations, especially the atomic-level observations of the long-range ordered atomic configurations and the local grain-boundary nanostructures using state-of-the-art analytical tools such as three-dimensional atom probe tomography (3D-APT) and Cs-corrected transmission electron microscopy (Cs-TEM), will be highlighted here.

Chemically complex ordered superlattice structure

Regarding realistic applications, the crystalline structures and atomic configurations matter fundamentally. Site occupation preferences of various elements and their alloying effects in various chemically complex intermetallic alloys or phases will be briefly discussed here. Representative examples of direct imaging of the sublattice occupation behavior by Cs-TEM and 3D-APT will also be presented.

Site occupation preference

Distinguished from the scenario in disordered alloys, elements in ordered alloys tend to regularly occupy specific sublattice sites. The elemental site preference can strongly influence the electronic bonding and therefore brings about numerous unique mechanical and functional properties. Over the past year, sub-

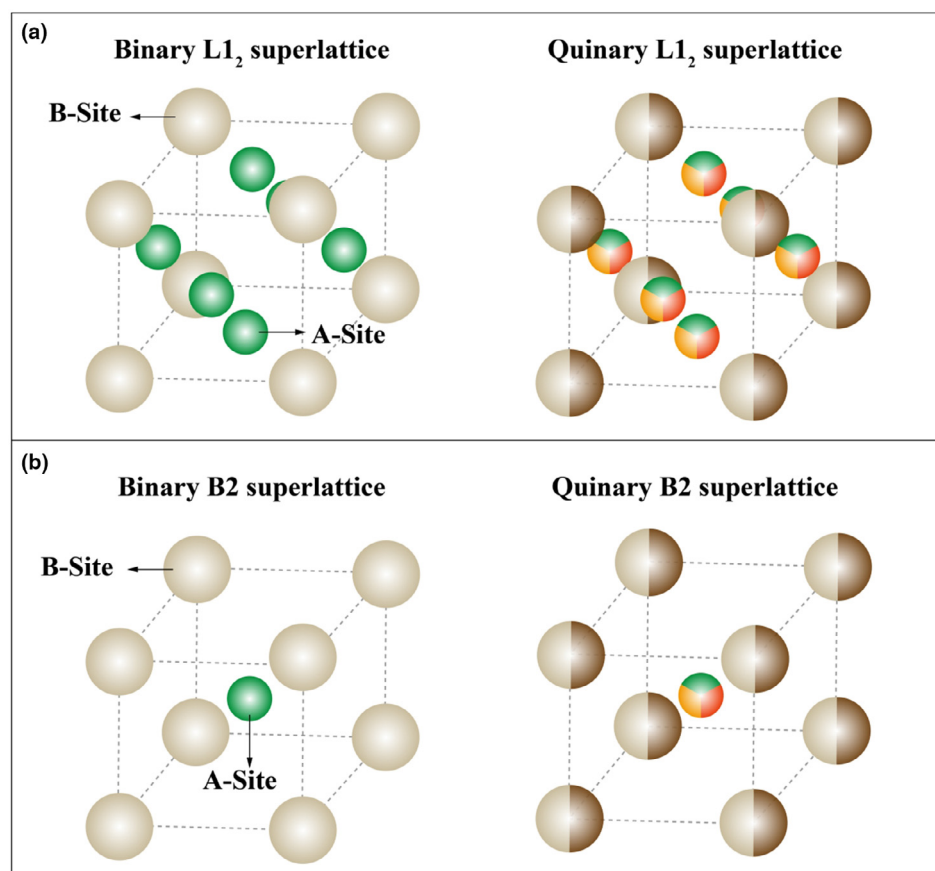


FIGURE 3

Schematic diagram of the unique atomic occupation behaviors of the novel (a) chemically complex L_{12} and (b) chemically complex B2 superlattices in comparison with the conventional binary counterparts. For the binary L_{12} /B2 structure, each sublattice is essentially occupied by one single element. By contrast, for the quinary L_{12} /B2 superlattice, each constituent sublattice is occupied by multiple elements. Tailoring the chemically complex sublattices with specific atom configurations are expected to change the properties of intermetallic materials significantly.

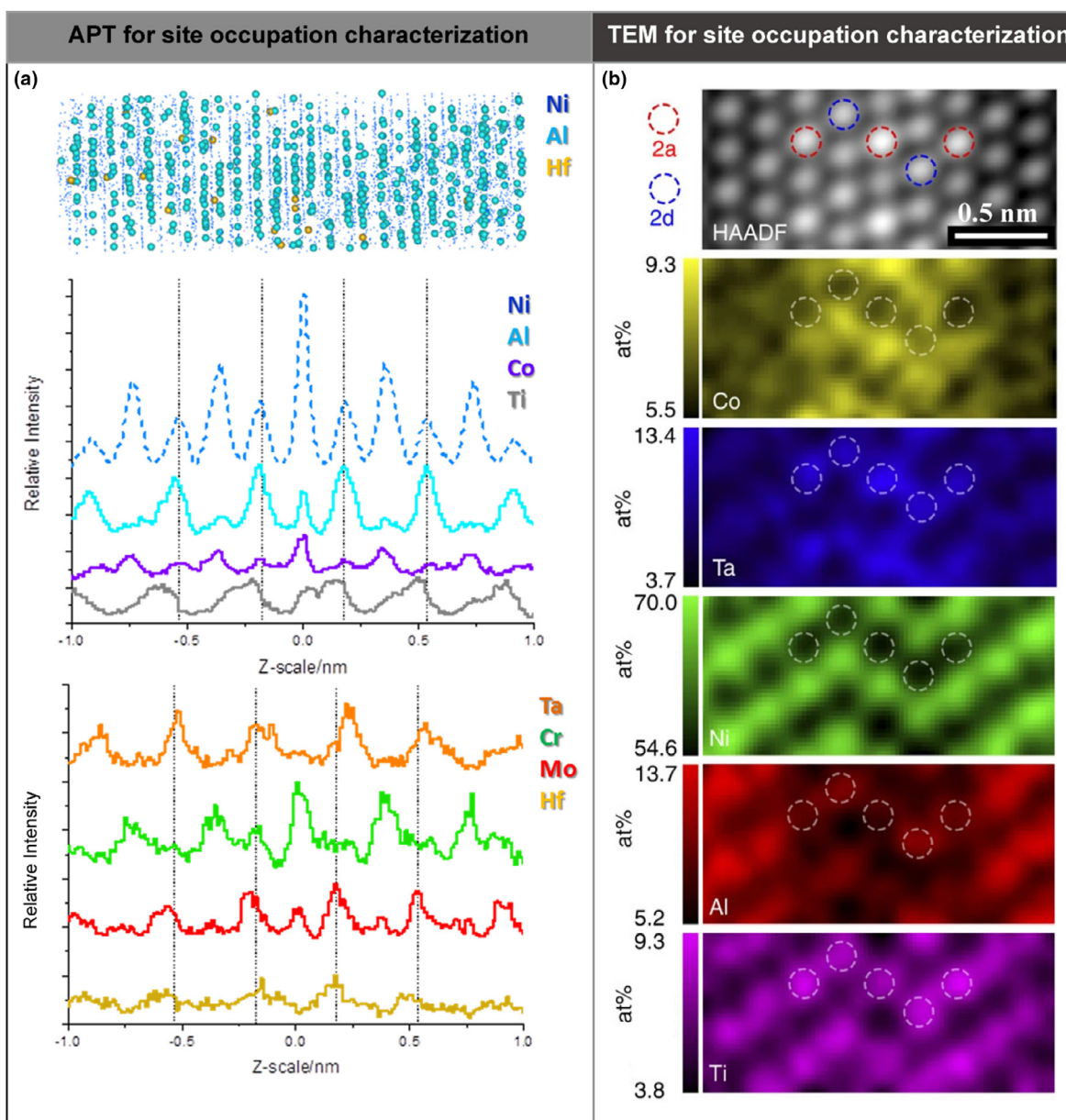
stantial research studies have been carried out to obtain an in-depth understanding of the atom site preference and the associated effect on the properties of the ordered intermetallic materials. In particular, the elemental occupation behaviors in the high-symmetry structures (cubic structures, such as L_{12} , B2, and L_{21} , etc) have attracted the most attention. Taking the L_{12} structure with the A_3B stoichiometry as an example, where A-site and B-site represent the face center and the corner positions, respectively. The site preference of an element is strongly composition-dependent. Schematic illustrations in Fig. 3a compare the atomic configuration between the conventional binary L_{12} -type structure and the quinary L_{12} -type CCIMA structure. As shown in Fig. 3b, a similar result can be identified in the B2-type superlattice structures. The fact of a more complex surrounding environment for individual elements makes the site occupation preference in the CCIMAs to be mysterious and intriguing. For example, in the binary Ni_3Al intermetallic alloy, the Cr element is suggested to occupy the B-sites as ternary addition [47], while it is observed to substitute A-sites in many of the multicomponent L_{12} phase [48,49]. Those unusual site preference behaviors of the CCIMAs may lead to a great potential of achieving unexpected properties. For example, Firstov et al.

showed that the $(TiZrHf)_{50}(CoNiCu)_{50}$ family of CCIMAs with the B2 ordering undergo the martensitic transformation and exhibit the shape-memory effect [50]. Liu et al. demonstrated that varying the element occupation in A-sites for the A_3B -type intermetallic materials plays an important role in controlling the phase structure and tuning the room-temperature ductility of intermetallic materials [13,23,51]. One of the typical examples is macro-alloying the hexagonally ordered Co_3V alloy with Fe and Ni elements [5]. The addition of Ni and Fe enables a crystallographic transition from the ordered hexagonal structure to cubic L_{12} structure, forming a new CCIMA with a composition of $(Co, Ni, Fe)_3V$. Compared to the extremely brittle Co_3V alloy, the resulting L_{12} -type CCIMA actually shows a significantly improved tensile elongation up to $\sim 40\%$. More recently, Ti is proved to remarkably increase the anti-phase boundary (APB) energy in a $(Ni, Co, Fe)_3(Al, Ti, Fe)$ -type CCIMAs, leading to the ultra-high tensile strength that outperforms most of the binary L_{12} -type intermetallic alloys [13]. Although the topic of site occupation preference has been extensively studied decades ago, the regulations of elemental occupation have never been fully clarified in the newly developed CCIMAs, which requires more systematic studies in the future.

Atomic-scale microstructural characterization

Regarding the atomic-scale microstructural characterization, the atomic site preference in intermetallic materials is generally analyzed theoretically utilizing first-principles and thermodynamic calculations. Yet for the CCIMAs, such a calculation requires a sharp increase in super-computer resources, and the corresponding computational capability, which is usually costly, time-consuming, may reduce the accuracy of the calculated results. With the improved modern techniques, especially the advent of Cs-TEM and 3D-APT, the site preference of each individual element now can be directly identified experimentally [52,53]. Fig. 4a shows a typical example of using 3D-APT for the charac-

terization of the site occupation. Elemental spatial distribution maps obtained from the successive {100} planes of the L_{12} phase allow a clear atomic distribution of each element [52]. Apparently, the elements of Al, Ti, Ta, Mo, and Hf prefer to reside on the B-sites. In contrast, Ni, Co, and Cr elements favor the A-sites. In addition, some researchers try to use a combination of Cs-corrected high-angle annular dark-field scanning transmission electron microscopy (HAADF-STEM) technique together with dispersive X-ray spectroscopy (EDX) with Super-X energy detector to experimentally identify the elemental site occupation probability at the atomic level. As shown in Fig. 4b, Smith et al. reveal the atomic configurations of a chemically complex η

**FIGURE 4**

(a) Spatial distribution maps produced by the 3D-APT plot the distribution of various solutes relative to the position of the Ni atoms in the L_{12} -type superlattice phase [52]. Each graph in this figure is generated by examining the local neighborhood around each individual Ni atom, building a frequency distribution of the relative separation in the $\langle 100 \rangle$ direction of the surrounding atoms. (b) Quantified atomic resolution EDX elemental maps at atomic scale of the chemically complex η phase which has formed at a two-layer stacking fault in the ordered L_{12} superlattice phase [53].

phase with a hexagonally ordered structure, where Ni and Co tend to occupy the A-sites, Ta and Nb preferentially occupy the Wyckoff 2a sites (red dashed circle), Al and Ti favor the Wyckoff 2d sites (blue dashed circle) [53]. Similar techniques have also been used to resolve the site occupation in many L1₂-type CCIMAs. Besides, another TEM technique with a basis of the orientation-dependence of characteristic X-ray emissions of alloying elements called for channeling-enhanced microanalyses, can be also used for the characterization of the site preference of such complex alloys [47].

Grain-boundary segregation and nanoscale phase transformation

Besides the ordered superlattice structure, multicomponent alloying will greatly change the localized microstructures at the vicinity of grain boundaries in the CCIMAs. In this section, we would like to highlight the recent advances in the quantification of grain-boundary chemistry and nanoscale phase transformation based on the state-of-the-art Cs-TEM and 3D-APT.

Grain-boundary segregation has long been a critical issue for the design of polycrystalline materials including ordered intermetallic alloys. For example, extensive studies have proved that boron atom can be strongly segregated to the grain boundary in conventional binary intermetallic alloys, such as Ni₃Al and NiAl, etc, which can significantly enhance the room-temperature ductility by improving the intrinsic cohesion of grain boundary or prevent water molecular reacting with active metal like Al [54–56]. Very recently, through the combined experimental analyses of the Cs-TEM and 3D-APT techniques, we demonstrated a novel toughening strategy in the L1₂-type CCIMAs via purposely engineering the grain-boundary disordered nanolayer (see Fig. 5a) [13]. The unique multielement co-segregation of Co, Fe, and B was clearly identified (see Fig. 5b), which surprisingly enables the destruction of the L1₂-type ordered superlattice and triggers the order-to-disorder phase transformation (i.e., the L1₂ to FCC transformation) in the vicinity of the grain boundaries. The resulting distinctive nanolayer acts as a sustainable ductilizing source, successfully preventing the CCIMA from brittle intergranular fractures by significantly enhancing dislocation mobilities [57]. It is interesting to point out that the 3D-APT technique provides a quantitative compositional analysis of the light elements (like boron) at the local grain-boundary region, which is extremely difficult to be achieved by using other conventional analytical tools. Nevertheless, underlying mechanisms behind the grain-boundary co-segregation and disordering behaviors in the CCIMAs are still far from being fully understood at the present time. It is believed that advances in various theoretical simulations may offer a great support in this regard.

Properties and application prospects

After carefully elaborating the unique microstructures of the CCIMAs, in this section, we would like to summarize the properties and prospects of CCIMAs for both structural and functional applications. Comparative analyses and corresponding discussions will also be provided.

Super-elastic and shape-memory effect

Metallic components with the ability to undergo large and reversible deformations over a broad temperature range are highly desirable for advanced engineering applications, such as deep-space and deep-sea exploration. However, as being governed by the yield stress and Young's modulus, the elastic strain limit rarely exceeds 1% due to the intrinsic limits of atomic bonding in traditional metals [58]. Fortunately, the controllable reversible martensitic transformation in the CCIMAs provides promising solutions to produce ultra-large and recoverable strain. Two main macroscopic effects have been characterized, that is, the super-elasticity and shape-memory effect [59]. The super-elasticity refers to the ability to recover from loading-originated large strains without significant residual strains. In contrast, the shape-memory effect refers to the capacity to recover to the original shape after being loaded with a temperature variation.

Conventional Cu-Al-based, NiTi-based, and Fe-based shape memory alloys exhibit up to a ~10% recoverable pseudo-elastic strain through the reversible stress-induced martensitic transformation [60,61]. For example, the crystal structure transformation between the ordered B2 structure and B19' structure enables the NiTi-based alloys with the ability to recover their original shapes when heated above the austenite finish temperature [62]. More recently, unprecedented super-elasticity has been successfully achieved in NiCoFeGa-based Heusler alloy with an ordered L2₁-type structure (see Fig. 6) [27]. Fig. 6a shows the overlapped stress–strain curves of the loading–unloading tests for the Co20 alloy (i.e., the Ni₃₅Co₂₀Fe₁₈Ga₂₇ alloy), where a maximum recoverable non-hysteretic super-elasticity of 15.2% combined with a high strength of ~1.5 GPa can be achieved. With the combined analyses of in-situ synchrotron X-ray diffraction and advanced scanning transmission electron microscopy (STEM) technique, such a large non-hysteretic super-elasticity response could be associated with a continuous phase transition between the disordered ω structure and ordered L2₁-type Heusler structure (see Fig. 6b–e) [27]. Moreover, no degradation of the reversible super-elasticity of the Co20 alloy can be observed after 8000 loading cycles over a wide temperature window (123 ~ 423 K), rendering it with a high elastic energy-storage capacity and cyclic stability.

More importantly, it should also be noted that a critical stress is necessarily required to induce the martensitic transformation, which usually increases with the increased temperatures as a result of the enhanced austenite stability [27]. Once the required critical stress exceeds the yield strength, plastic deformation occurs ahead of the reversible martensitic transformation, rendering the disappearance of super-elasticity. Such an issue sets a limit to the temperature range for super-elasticity and restricts the engineering applications of shape-memory alloys. Luckily, the vast compositional space of CCIMAs provides a feasible approach to exclude the temperature effect. For example, through carefully compositional tuning, Fe–Mn–Al–Cr–Ni-based shape memory alloys with a temperature-independent critical stress were designed, in which B2-type intermetallics are believed to play an important role in facilitating the thermoelastic martensitic transformation [63,64]. Zarnetta et al. [65] reported a Ti–Ni–Cu–Pd CCIMA with near-zero thermal hysteresis and

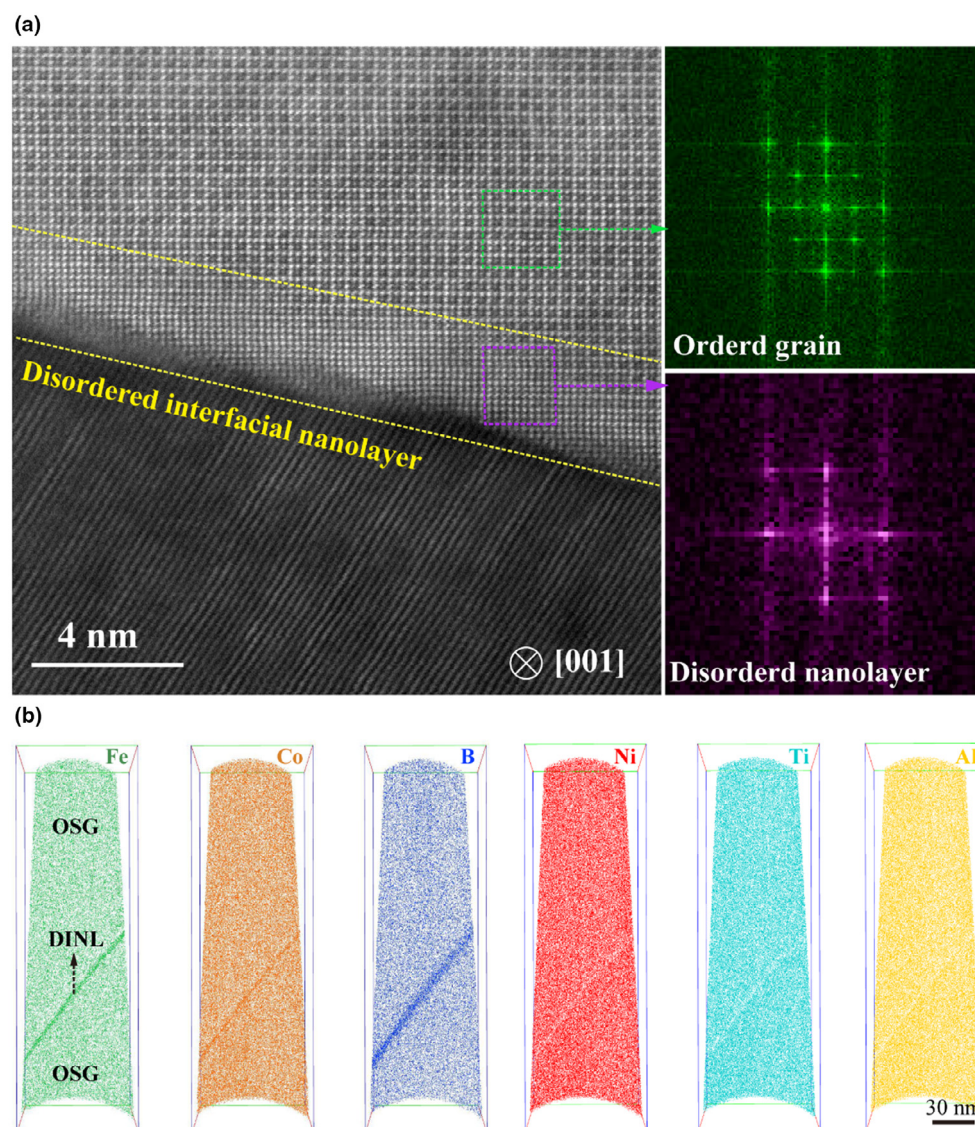


FIGURE 5

Nanoscale disordering and multi-element co-segregation in the vicinity of grain boundaries of the $\text{Ni}_{43.9}\text{Co}_{22.4}\text{Fe}_{8.8}\text{Al}_{10.7}\text{Ti}_{11.7}\text{B}_{2.5}$ (at.%) superlattice alloy [13]. (a) High-resolution HAADF-STEM image and the corresponding fast Fourier transform (FFT) patterns reveal the ultrathin disordered layer at the grain boundaries with a nanoscale thickness. (b) Atom maps reconstructed using 3D-APT that show the distribution of each element. Fe, Co, and B are enriched at the disordered interfacial nanolayer (DINL), whereas Ni, Al, and Ti are enriched in the ordered superlattice grain (OSG) correspondingly.

excellent functional stability. They found that the degree of interfacial coherency between the B2 phase and the transformed orthorhombic martensite plays a dominant role. By carefully tailoring the Ni:Pt ratio, the geometric compatibility of these two phases has been optimized, which in turn results in a minimum increment of the bulk energy and thus leads to a decrease in the width (approach zero) of the thermal hysteresis. Moreover, Piorunek et al. studied the chemical complexity effect on the solidification microstructures and martensitic transformations of a high-entropy shape-memory alloy (HESMA) system. They discovered a novel B2-type NiCuPdTiZrHf HESMA, which has the potential to provide maximum shape memory strains close to 15% [66].

Strength-ductility combination at ambient temperature

The strong chemical bonding of long-range ordered intermetallic alloys makes them attractive to be developed as advanced structural materials with superior strengths. However, as the crystalline structures become highly ordered, brittle failure is more likely to take place under external loading (especially the tension condition) and demolish the most desirable properties of this class of alloys [67]. Recent studies have demonstrated that extraordinary strength-ductility balance at ambient temperature can be successfully realized in the novel L1_2 -type CCIMA by triggering the multi-element co-segregation and associated nanoscale interfacial disordering at grain boundaries [13]. Apart from the eliminated intergranular embrittlement, the yield strength

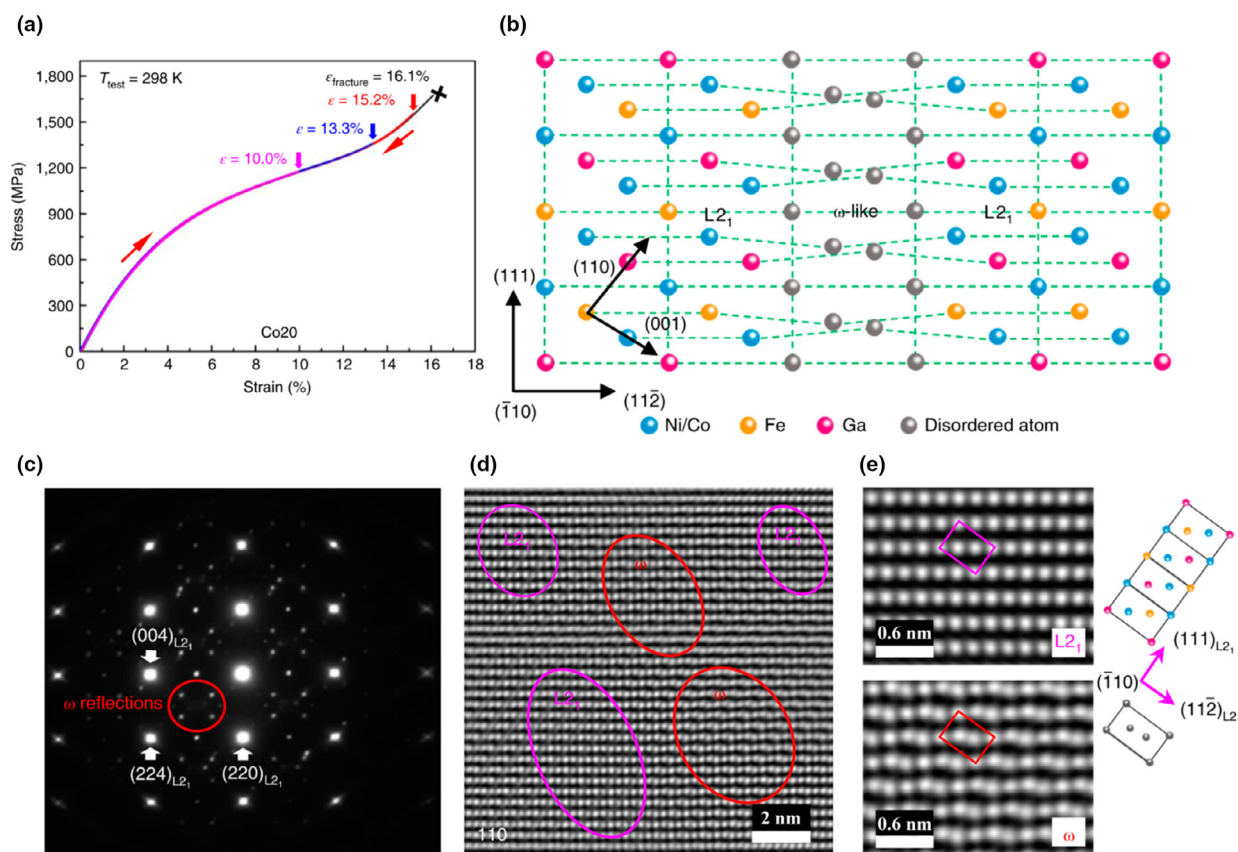


FIGURE 6

Unprecedented super-elasticity and unusual phase transformation behaviors in the $\text{Ni}_{35}\text{Co}_{20}\text{Fe}_{18}\text{Ga}_{27}$ (at.%) CCIMA (single-crystal state) [27]. (a) Stress-strain curves at room temperature, showing unprecedented super-elasticity with a recoverable strain up to 15.2% and a high fracture strength of 1.6 GPa. (b) Schematic diagram of the ordered L_{21} and disordered ω structures. (c) Corresponding selected area diffraction pattern with reflections from both L_{21} and ω structures. (d and e) Inverse Fast Fourier Transformation (IFFT) image of the L_{21} and ω structures.

of the L_{12} -type CCIMA ($\text{Ni}_{43.9}\text{Co}_{22.4}\text{Fe}_{8.8}\text{Al}_{10.7}\text{Ti}_{11.7}\text{B}_{2.5}$, at.%) also exceeds 1 GPa, which is 2.6 times higher than that of simple Ni_3Al -based alloys (Fig. 7a). The substantially enhanced strength can primarily be ascribed to the increased APB energy via multiple alloying additions. The occupation of Al sublattice sites in Ni_3Al -type L_{12} intermetallic alloy by Ti atoms substantially increases the APB energy [68], and thereby increases the macroscopic flow stress of the current CCIMA by elevating the energy barrier required for the leading dislocation bowing out. The APB energy of this CCIMA has been estimated to be $\sim 296 \text{ mJ/m}^2$, whereas that of binary Ni_3Al alloy is only $\sim 110 \text{ mJ/m}^2$ [69]. Therefore, as compared to the Ni_3Al alloy, the extra APB energy accounts for an increment in the critical stress ($\sim 722 \text{ MPa}$) required for the dislocation nucleation in this NiCoFeAlTi-type CCIMA, resulting in exceptionally high strengths during tensile deformation.

The larger tensile ductility can be attributed to the formation of the unique grain-boundary disordered nanolayer driven by the multi-element co-segregation, which is effective in suppressing the intergranular fracture. As shown in Fig. 5, the enrichment of Fe, Co, and B are identified in the vicinity of grain boundaries, and thereby promotes the FCC-type solid-solution structure formation by destabilizing the ordered L_{12} structure. During plastic deformation, such disordered interfacial nanolayers play an

important role in eliminating possible intergranular embrittlement, which is generally considered as the main concern of polycrystalline ordered superlattice alloys for engineering applications [20,70]. In brief, the macroscopic mechanical properties of this CCIMA would benefit from the formation of the grain-boundary disordered nanolayer in the following two aspects. First, the grain-boundary disordering reduces the critical stress for dislocation generation and allows an easier dislocation transmission between neighboring grains. It should be noted that, for the L_{12} -type ordered superlattice, the emission of dislocation from a crack tip requires an additional energy barrier [57]. With the interfacial disordering, such an energy barrier and the susceptibility for crack initiation and propagation along grain boundaries will be removed. Second, the nanoscale disordered layer can act as a ductile buffer zone that helps to relieve the localized stress concentration at grain-boundary regions when plastically deformed. This can be supported by Fig. 7c and d, where massive dislocations were operative in the vicinity of disordering nanolayer decorated boundary without intergranular cracking. Therefore, the ductile multicomponent disordered layer ensures the plastic deformation compatibility between neighboring ordered grains and therefore suppresses the potential microcrack formation along grain boundaries even at a high-strength level (see Fig. 7b and c). These two above-

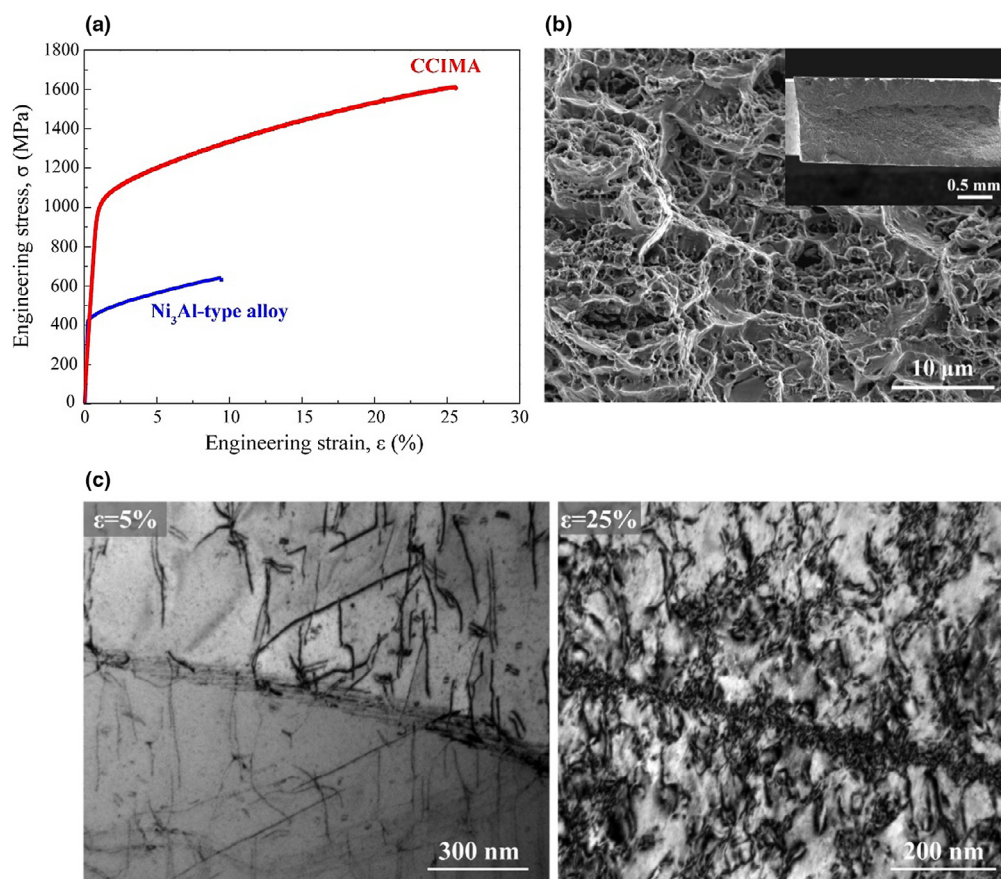


FIGURE 7

Excellent room-temperature tensile properties and ductile fracture behaviors of the L_{12} -type $\text{Ni}_{43.9}\text{Co}_{22.4}\text{Fe}_{8.8}\text{Al}_{10.7}\text{Ti}_{11.7}\text{B}_{2.5}$ (at.%) CCIMA with grain-boundary disordered nanolayer [13]. (a) Representative room-temperature tensile stress–strain curve, showing pronounced strength–ductility synergy in comparison with the chemically simple Ni_3Al -type alloy. (b) Corresponding tensile fractography showing dimple formation. (c) TEM images of the plastically deformed specimens (5% and 25% strained), demonstrating pronounced dislocation activities can be accommodated at grain boundaries without intergranular crack formation and associated embrittlement.

mentioned benefits contribute to a large tensile ductility and associated pronounced strain-hardening capacities for the L_{12} -type CCIMA with nanoscale grain-boundary disordering.

Another critical issue for CCIMAs to be used as structural materials is the susceptibility to extrinsic environmental embrittlement. Previous studies indicated that many polycrystalline intermetallic systems are susceptible to the moisture-induced embrittlement along the grain boundaries [20]. Atomic hydrogen released from the chemical reaction of water vapor with the active elements (such as the Al) severely embrittle the alloys and leads to the poor ductility and intergranular cracking. Alloying addition of Fe has also been reported to alleviate the propensity for environmental embrittlement of the Ni_3Al -based alloys [56]. It should also be noted that the embrittling agent at elevated temperatures is oxygen by dynamically penetrating along grain boundaries when mechanically loaded [71]. Alloying with 8 at.% Cr to Ni_3Al -based intermetallic alloy eliminates such dynamic environmental embrittlement in the temperature range between 600 and 800 °C, which is associated with the rapid formation of protective chromium oxide films and the reduced propensity for oxygen to penetrate along grain boundaries at elevated temperatures [72]. Luckily, the vast compositional space and numerous elemental combinations among CCIMAs are

expected to offer a feasible solution to conquer the adverse extrinsic embrittlement effect via beneficial alloying additions [13].

Thermal stability and creep resistance at elevated temperatures

The highly ordered crystal structure gives rise to low atomic mobility and sluggish diffusion in intermetallic alloys, all of which make them attractive for structural applications at elevated temperatures with superior microstructural stability. The Ni_3Al phase with the L_{12} structure plays an important role in the strengthening of Ni-based superalloys by impeding dislocation movement. Such unique property drives extensive studies on developing Ni_3Al -based intermetallic alloys for advanced high-temperature applications. In the 1980s, Oak Ridge National Laboratory launched a research program by focusing on Ni_3Al -based intermetallic alloys [73]. Given the beneficial effects of the anomalous positive temperature dependence of the yield strength as well as superior high-temperature wear and oxidation resistance, a series of Ni_3Al -based intermetallic alloys were developed for industrial purposes [72]. For example, as derived from Ni_3Al , IC-211M alloy (Ni–15.9Al–8.0Cr–0.8Mo–1.0Zr–0.03B, at. %) has been extensively used as transfer rolls in furnaces, the

application of which has been estimated to bring in saving of 25 million dollars per year [74].

The discovery of L_{12} -type precipitates among ternary Co-Al-W alloys also drives a series of researches on investigating the thermo-physical properties of $Co_3(Al,W)$ -based intermetallic alloys [75]. Unlike the Ni_3Al phase which is thermodynamically stable up to 1300 °C, the ternary $Co_3(Al,W)$ phase is metastable, which decomposes into B2-CoAl and DO_{19} - Co_3W phases after long-term annealing at 900 °C [76]. Guided by first-principle calculations, several beneficial alloying additions have been identified for the improved thermal stability, e.g., Ni, Ti, and Ta [77]. Recently, a multicomponent $(Co,Ni)_3(Al,W,Ti,Ta)$ -type CCIMA with a nominal composition of $Co_{46.9}Ni_{30}Al_{11}W_{5.5}Ti_4Ta_{2.5}B_{0.10}$ (at.%) was developed along with this line of thinking (Fig. 8a), which demonstrated the superior high-temperature phase stability with a solvus temperature of 1296 °C (Fig. 8b) [26]. Apart from the significantly enhanced thermal stability, this new kind of $(Co,Ni)_3(Al,W,Ti,Ta)$ -type CCIMA also demonstrated pronounced yield strength anomaly (compression test) as the defor-

mation temperature increases from 250 to 800 °C, with a peak yield strength of ~ 700 MPa (Fig. 8c). Moreover, the steady-state creep rate of this $(Co,Ni)_3(Al,W,Ti,Ta)$ -type CCIMA is more than an order of magnitude smaller than that of conventional Ni_3Al -based intermetallic alloys (Fig. 8d), suggesting a much superior creep resistance at elevated temperatures.

Rapid grain coarsening at elevated temperatures sets another severe limitation for the high-temperature application of polycrystalline materials. Remarkably, the CCIMAs with nanoscale disordered interfaces demonstrated exceptional grain coarsening resistance with negligible grain growth even after annealing at 1050 °C for 120 h [13]. The multiple elements within the grain-boundary disordered layer increased the configuration entropy and lowered the Gibbs energy of grain boundaries, which reduced the driving force for grain coarsening. Moreover, the solubility of each element varied between grain boundaries and grain interior, leading to the retarded solute diffusion between adjacent grains and associated restricted grain-boundary motion. The local enrichment of constituent elements

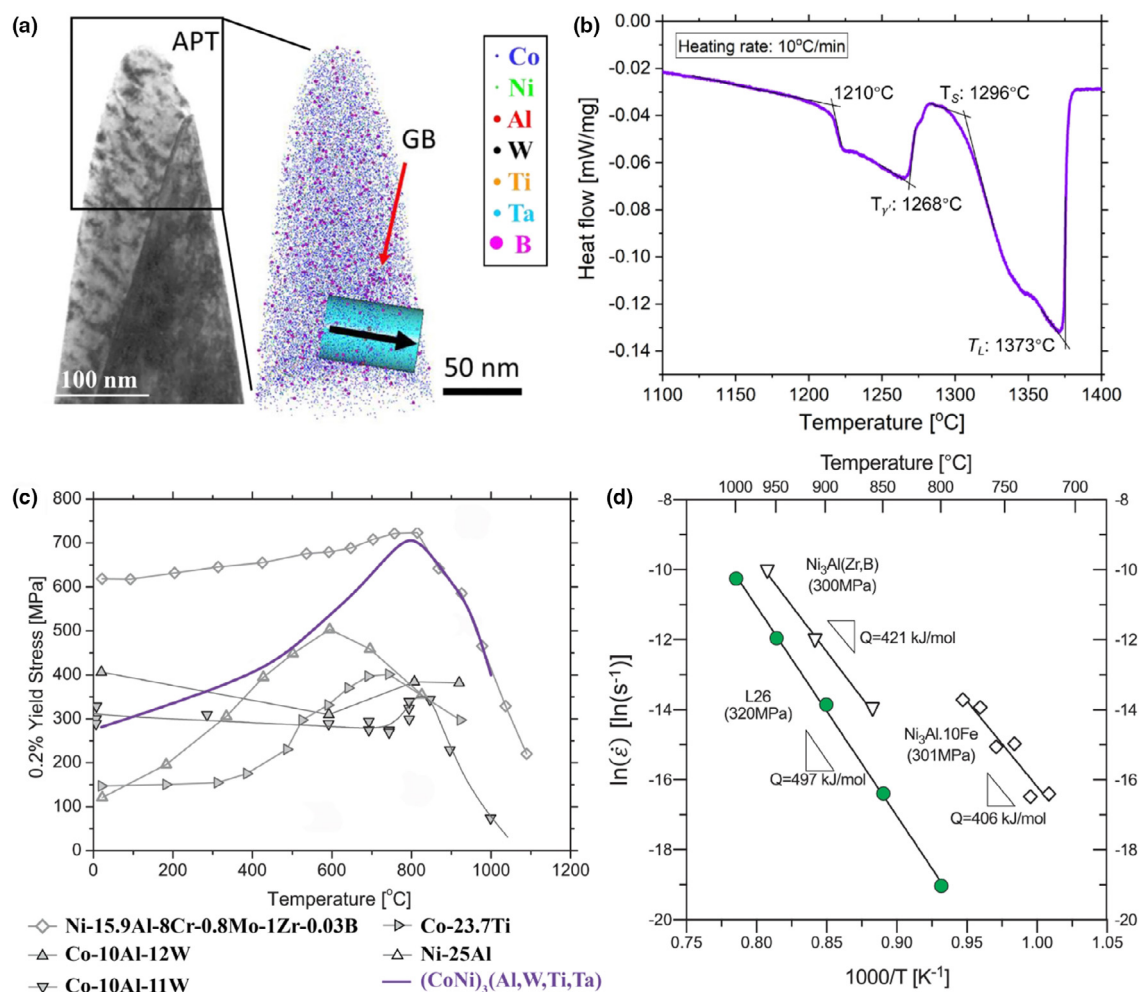


FIGURE 8

The chemistries and mechanical properties of the $(Co,Ni)_3(Al,W,Ti,Ta)$ -type CCIMA with a composition of $Co_{46.9}Ni_{30}Al_{11}W_{5.5}Ti_4Ta_{2.5}B_{0.10}$ (at.%) [26]. (a) BF-TEM image and the corresponding reconstructed APT nanotip of this L_{12} -type CCIMA. (b) A differential scanning calorimetry heating curve of this CCIMA, indicating a solvus temperature of 1296 °C. (c) The plot between yield strength and deformation temperature, showing a pronounced yield strength anomaly behavior. (d) Arrhenius plot of strain rate vs. temperature for this kind of CCIMA (L26 alloy) deformed under a constant stress of 320 MPa (denoted by green dots), demonstrating superior creep resistance for this multicomponent L_{12} -type CCIMA.

at grain boundaries also gave rise to the kinetic stabilization of grain by the solute-drag effect [78]. All these factors may contribute to the inhibited grain growth at elevated temperatures, suggesting the promising outlook for polycrystalline CCIMAs to be used as high-temperature structural materials.

Novel functional properties

Besides being used as advanced structural materials, the CCIMAs have been demonstrated to exhibit excellent functional performance as electrochemical catalysts, thermoelectric materials, superconductors, and magnetocaloric materials. Some representative examples of success will be discussed in this section.

Electrochemical water splitting has been identified as a particularly promising and appealing technology for hydrogen productions. Through melt-spinning and dealloying techniques, Jia et al. developed a novel high-performance cost-effective L1₂-type FeCoNiAlTi CCIMA [79]. The optimized CCIMA dealloyed by 15 h shows the excellent hydrogen evolution reaction (HER) performance of the dealloyed CCIMA in alkalinity condition, rendering a low overpotential of 88.2 mV at a current density of 10 mA cm⁻² and a small Tafel slope of 40.1 mV dec⁻¹. Such impressive performance stands at a comparable level with those noble catalysts like Pt-contained catalysts, surpassing most of the previous non-noble catalysts reported [80]. They demonstrated that the underlying mechanisms behind such superior performance are twofold. On one hand, the multicomponent nature of the CCIMAs leads to a strong chemical synergistic effect on the alteration of the electronic structure. On the other hand, it also allows greater opportunity for better optimization of the electrocatalytic performance by isolating the active elements in the ordered superlattice. More specifically, due to the existence of two kinds of sublattice, one single Al atom on A-type sublattice coordinated with another element on the B-type sublattice is suggested to provide a beneficial Gibbs free energy (ΔG_{H^+}) value for the Heyrovsky step with the H_{ad} adsorption and desorption, which can be well-achieved in the FeCoNiAlTi CCIMA due to the specific site-occupation preference of individual elements.

Likewise, the CCIMAs have been also demonstrated as good catalysts for other chemical reactions like oxygen evolution reaction (OER), and electrodes reaction for lithium battery, etc. Ding et al. reported a Laves-type quinary CCIMA wrapped with an ultrathin amorphous high entropy oxide for the OER process, which exhibited a low overpotential (0.288 V@10 mA cm⁻²) and excellent durability for 30 h [81].

In addition, some CCIMAs also show great potential in thermoelectric, superconductor, and refrigeration applications. For example, Jiang et al. designed one n-type Pb–Sn-based CCIMA formed by entropy-driven structural stabilization, which showed a remarkable improvement in the figure of merit (zT) value (1.8 at 900 K) and conversion efficiency (12.3% at $\Delta T = 507$ K) [82]. They reported that the largely distorted lattice in the CCIMA causes unusual lattice strain, which leads to a strong scattering for heat-carrying phonons and boosts the heat-conversion efficiency of the materials. Similarly, Yan et al. fabricated the NbFeSb-based half-Heusler CCIMAs by arc melting and subsequent spark plasma sintering [83]. It was reported that by increasing the content of the alloying element to substitute Nb-site, the thermal conductivity decreases (down to 2.5 W/mK), while the

figure of merit (zT) value increases (0.88 at 873 K). In addition, inspired by complex copper oxide with superior superconducting performance, Cava and coworkers reported a single-phase quaternary LnNi₂B₂C CCIMA with a high superconducting temperature up to 16.6 K [84]. Via reactive indium flux method, Bao et al. prepared Y₇Ru₄InGe₁₂ single crystal, which exhibits superconductivity with a transition temperature of ~5.8 K [85]. The large superconducting specific-heat jump induced by electron-phonon coupling suggested that attempts of combining rare-earth and transition-metal elements are potential to obtain superconductivity. Furthermore, many Heusler-type CCIMAs exhibit a giant magnetocaloric effect for refrigeration applications. Qu et al. reported Ti-doped quinary NiTiCoMnSn intermetallic system [86]. The results show that Ti addition brings about a large magnetic entropy change (18.7 J kg⁻¹ K⁻¹ under 5 T) and reversible room-temperature magnetocaloric effect.

Outlook and future work

As a newly emerged field in materials science, the CCIMAs offer a rich playground for designing novel materials for structural applications because of their tunable superlattice structures, huge compositional ranges, and promising mechanical properties. Along with the deepened studies gradually, the application prospect of CCIMAs would become more brilliant and broader, and meanwhile, new challenges arise accordingly, especially upon the innovative alloy design and manufacturing techniques. Therefore, more fundamental and comprehensive studies should be carried out systematically to further accelerate the discovery of novel high-performance CCIMAs, and ultimately, facilitate their wide applications in different industrial fields. Here, we briefly outline below several critical issues and possible key directions for future research on advanced structural CCIMAs.

High-throughput design of ordered superlattice structure

In general, the optimal design of CCIMAs, as novel alloys, is indeed complicated, since it must be considered comprehensively about many critical issues including both the microstructures and properties. The increased number of constituent elements greatly enlarges the compositional space for material exploration, which however, makes it is extremely difficult for us to quickly screen out the desired alloys with specific structures. A major impediment is the lack of comprehensive understanding of the physical metallurgy mechanisms in such complex alloy systems. First, it is crucial for us to establish a quantitative prediction of the composition dependence of sublattice occupancies and the role of atomic bonding states for various CCIMAs. Moreover, the well-targeted quantitative “grain boundary design” in CCIMAs has remained elusive until now, both theoretically and experimentally. While some advances have been made in the grain-boundary engineering technology [87–89], the ability to predict the elemental segregation preference and the associated phase transformation rules for a given CCIMAs still remains at the qualitative and empirical level, which poses a major challenge to materials scientists for designing alloys with customized properties.

More importantly, it is worthy to note that the conventional trial-and-error method is time-consuming and labor-intensive,

which becomes increasingly difficult for alloying screening in the chemically complex systems. With the rapid development of machine learning approaches with intelligent data mining and database construction, the high-throughput computational design may offer a reliable and efficient tool to explore the enormous space of promising materials [90–92]. In the future, more efforts and attempts should be made in this aspect, helping to accelerate the discovery of high-performance CCIMAs. Additionally, from the perspective of economic and resource availability, sustainable alloy design should also be taken into a serious consideration in the metallurgical community [93–96]. Indeed, using a large number of elements makes sense only if they are widely available markets dependent on the geographic concentration and coupled production. However, recycling of chemically complex alloys is generally difficult excepted if they can be re-used as they are. As a result, besides the continuous performance optimization by elaborately tailoring the compositions of CCIMAs, it is necessary for metallurgical designers to effectively incorporate alloying screening criteria (such as the price, availability, and recyclability) based on the economic and resource use consequences of element selection [93].

Microstructural control and mechanical properties at elevated temperatures

The long-term thermal stability at elevated temperatures fundamentally determines the working temperature range and engineering reliability of these novel CCIMAs. Interestingly, recent studies have reported that several promising CCIMAs are highly stable at high temperatures, which endows them with great potential as a new kind of excellent heat-resistant materials [13,28]. Nevertheless, due to the chemical complexity induced by the multiple elements and their mutual interactions, phase decomposition of the ordered superlattice might take place during long-term exposures under various temperatures. Noted that the undesired precipitation of brittle phases, like the deleterious topologically close-packed (TCP) phases, will cause performance degradation of bearing capacity and durability [97]. Therefore, to achieve the better microstructural control, it is essential for us to carefully evaluate the microstructural evolutions of various CCIMAs in different temperature ranges, and meanwhile, quantify the alloying effects of the constitutive elements on their long-term stability. Moreover, as we discussed above, the grain-boundary structure, such as grain-boundary segregation, phase precipitation, character and distribution, could have a big influence on the performance of materials [49,87,88]. Previous studies have explored how to tune the local chemistries and nanostructures at the vicinity of grain boundaries for preventing intergranular embrittlement [13]. As a result, another important question is, “what is the thermal stability of grain-boundary structures in the CCIMAs?”. In general, as compared to the grain interior, microstructural evolutions at the grain boundaries will become more complicated, and more studies are necessarily needed to fundamentally understand them. On the other hand, not unnaturally, the high-temperature tensile behavior, creep and fatigue resistance, as well as the associated deformation micro-mechanisms should be systematically investigated, with the emphasis on establishing the composition-microstructure-processing-property relationship in this class of CCIMAs. In addition,

more attention should be paid to high-temperature structural applications of single crystals and directionally solidified CCIMAs.

Designing high-performance nanocrystalline CCIMAs for structural applications

Compared to the coarse-grained materials, the nanocrystalline materials with extremely fine grain sizes at the nanometer level may exhibit many exceptional physical and mechanical properties, such as ultrahigh strength/hardness, improved toughness, reduced elastic modulus, enhanced thermal expansion coefficient, etc. [98–101]. Keeping this incentive in mind, extensive studies have been conducted in these areas. However, two major weaknesses of most nanocrystalline materials, i.e., the strong coarsening tendency and room-temperature brittleness (very limited tensile ductility), seriously hinder their structural use in practical engineering fields [102]. In view of the possible unusual structural features of CCIMAs, especially the unique composite architecture of the ordered grain with disordered grain boundary nanolayer, it is believed that novel high-strength ultrafine-grained or nano-grained with enhanced thermal stability and strength-ductility combination could be achieved based on the CCIMAs strategy. Take the $L1_2$ -type CCIMAs for example, in comparison with the conventional solid-solution alloys, the long-range superlattice structures generally provide a strong chemical binding with lower atomic mobility and diffusivity, all of which will contribute to their improved thermal stability at elevated temperatures. More importantly, by manipulating the local chemistry and phase transformation at grain boundaries, the thermodynamically stable disordered nanolayers between adjacent ordered grains would be introduced controllably, which are expected to substantially prevent the grain coarsening while improving their ductility. Fig. 9 schematically illustrates the conceptual design of stable nanograined CCIMAs in the future. At present, however, despite some promising preliminary results, research in this regard is still in an early stage

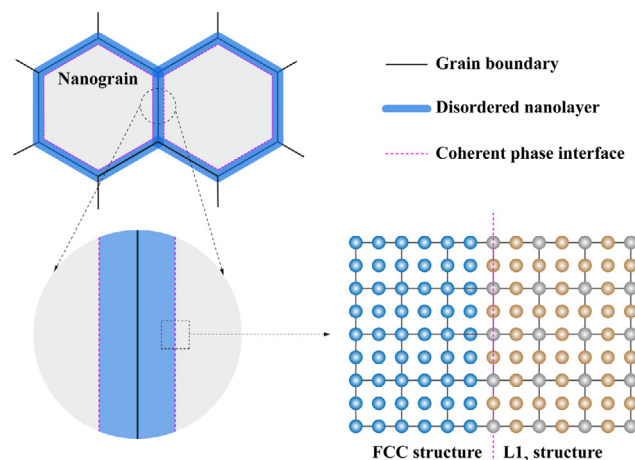


FIGURE 9

Schematic illustration of the conceptual design of stable nanograined CCIMAs in the future. The presence of thermodynamically stable FCC-type nanolayer at the grain boundaries, which shows coherent interfaces with the surrounded $L1_2$ superlattice, are expected to effectively pin the boundaries for grain-size stabilization.

and not comprehensive enough. Therefore, in the future, with the advanced technologies developed for the processing and characterizations, it is imperative for us to fabricate various kinds of bulk ultrafine-grained or nanocrystalline CCIMAs and extensively investigate their mechanical properties, as well as the associated physical micro-mechanisms.

Concluding remarks

It is well known that those who dominate the new materials dominate the future's high-end technology. The concept of CCIMAs represents a new and promising frontier for the innovative design of novel materials and devices. In the present work, we critically reviewed the recent major new ideas and key accomplishments in the design principles, microstructural characterizations, and intriguing properties of CCIMAs. As a newly emerged metallic material, several CCIMAs with long-range ordered superlattice structures composed of various multiple alloying elements have been demonstrated with many novel and unprecedented properties and thus they are being actively explored for numerous promising applications, in particular for advanced structural applications. The combinatorial approaches including the state-of-the-art microanalysis techniques (such as the 3D-APT) and theoretical simulations (such as the DFT first-principles calculation) play crucial roles in revealing their intrinsic metallurgical behaviors. Inspired by these attractive findings, we believe that more and more novel high-performance metallic materials with superb structural/functional properties can possibly be discovered based on the chemically complex intermetallic systems. Despite these advances, however, research on this topic is in its infancy at present, and still, there are many unaddressed critical issues and challenging work. In the near future, to further speed up the well-targeted quantitative design and controllable fabrication of CCIMAs with optimized properties, significant effort should be devoted to fundamentally elucidating the alloying behaviors and associated microstructural evolutions of CCIMAs, as well as the atomistic mechanisms behind them. Moreover, to promote their large-scale industrialization, more attention should be paid to the new high-throughput experimental work to systematically evaluate their microstructure-sensitive properties under various service conditions, especially under harsh environments like high temperatures, cryogenic temperatures, high-energy irradiation, etc. It is undoubtedly that the CCIMAs strategy indeed significantly widens the dimension for alloy design with target properties, which is expected to be an appealing pathway for developing novel high-performance materials and devices.

Declaration of Competing Interest

The authors declare that they have no known competing financial interests or personal relationships that could have appeared to influence the work reported in this paper.

Acknowledgements

T. Yang and C.T. Liu from City University of Hong Kong (CityU) are grateful for the financial support from the Hong Kong Research Grant Council (RGC) with CityU Grant 9610498, 11213319, and 21205621. T. Yang also thanks the financial support from Hong Kong Institute for Advanced Study (Grant

9360157), CityU Shenzhen Research Institute (SRI) (Grant 2020A1515110647), and National Natural Science Foundation of China (NSFC) (Grant No. 52101151). Y.L. Zhao is grateful for the financial support from NSFC (Grant No. 52101135). We especially appreciate the invitation from J. Lou who provides us a good opportunity to better advance this important and interesting research area. The authors declare no conflict of interest.

References

- [1] C.T. Liu et al., *Ordered intermetallics: physical metallurgy and mechanical behaviour*, Springer Science & Business Media, 2012.
- [2] N.S. Stoloff, V.K. Sikka, *Physical metallurgy and processing of intermetallic compounds*, Springer Science & Business Media, 2012.
- [3] D.P. Pope, *MRS Online Proc. Libr. Arch.* (1986) 81.
- [4] C.T. Liu, J. Stiegler, *Science* 226 (4675) (1984) 636, <https://doi.org/10.1126/science.226.4675.636>.
- [5] C.T. Liu, *Int. Met. Rev.* 29 (1) (1984) 168, <https://doi.org/10.1179/imtr.1984.29.1.168>.
- [6] K. Gschneidner Jr et al., *Nat. Mater.* 2 (9) (2003) 587, <https://doi.org/10.1038/nmat958>.
- [7] D.P. Pope, R. Darolia, *MRS Bull.* 21 (5) (2013) 30, <https://doi.org/10.1557/s088376940003548x>.
- [8] S.C. Deevi, *Prog. Mater. Sci.* (2020), <https://doi.org/10.1016/j.pmatsci.2020.100769>.
- [9] R. Mitra, Wanhill, R., *Structural intermetallics*, in: *Aerospace materials and material technologies*, Springer (2017), pp 229.
- [10] R.D. Noebe et al., *The physical and mechanical metallurgy of NiAl*, in: *Physical metallurgy and processing of intermetallic compounds*, Springer, 1996, p. 212.
- [11] C.G. McKamey et al., *J. Mater. Res.* 6 (8) (2011) 1779, <https://doi.org/10.1557/jmr.1991.1779>.
- [12] J.H. Perepezko, *Science* 326 (5956) (2009) 1068, <https://doi.org/10.1126/science.1179327>.
- [13] T. Yang et al., *Science* 369 (6502) (2020) 427, <https://doi.org/10.1126/science.abb6830>.
- [14] N. Stoloff, *Int. Mater. Rev.* 34 (1) (1989) 153, <https://doi.org/10.1179/imr.1989.34.1.153>.
- [15] H. Clemens, S. Mayer, *Adv. Eng. Mater.* 15 (4) (2013) 191, <https://doi.org/10.1002/adem.201200231>.
- [16] S.-J. Liang, D. Pope, *Acta Metall.* 25 (5) (1977) 485, [https://doi.org/10.1016/0001-6160\(77\)90188-2](https://doi.org/10.1016/0001-6160(77)90188-2).
- [17] Z.M.T. Chen et al., *Scr. Mater.* 121 (2016) 28, <https://doi.org/10.1016/j.scriptamat.2016.04.029>.
- [18] D.-M. Wee et al., *Trans. Jpn. Inst. Metals* 21 (4) (1980) 237, <https://doi.org/10.2320/matertrans1960.21.237>.
- [19] A.M. Russell, *Adv. Eng. Mater.* 5 (9) (2003) 629, <https://doi.org/10.1002/adem.200310074>.
- [20] C.T. Liu et al., *Scr. Metall.* 23 (6) (1989) 875, [https://doi.org/10.1016/0036-9748\(89\)90263-9](https://doi.org/10.1016/0036-9748(89)90263-9).
- [21] O. Izumi, T. Takasugi, *J. Mater. Res.* 3 (3) (1988) 426, <https://doi.org/10.1557/JMR.1988.0426>.
- [22] K. Aoki, *Mater. Trans. JIM* 31 (6) (1990) 443, <https://doi.org/10.2320/matertrans1989.31.443>.
- [23] A. Chiba et al., *Improvement in ductility of Ni₃Al by γ former doping*, in: *High Temperature Aluminides and Intermetallics*, Elsevier, 1992, p. 108.
- [24] M. Matsuda et al., *J. Mater. Sci.* 46 (12) (2011) 4221, <https://doi.org/10.1007/s10853-010-5236-3>.
- [25] T. Takasugi et al., *Acta Metall. Mater.* 38 (5) (1990) 747, [https://doi.org/10.1016/0956-7151\(90\)90026-D](https://doi.org/10.1016/0956-7151(90)90026-D).
- [26] F.R. Long et al., *Acta Mater.* 196 (2020) 396, <https://doi.org/10.1016/j.actamat.2020.06.050>.
- [27] H. Chen et al., *Nat. Mater.* 19 (7) (2020) 712, <https://doi.org/10.1038/s41563-020-0645-4>.
- [28] K. Yao et al., *Scr. Mater.* 194 (2021), <https://doi.org/10.1016/j.scriptamat.2020.113674>.
- [29] S. Wang et al., *Mater. Design* 168 (2019), <https://doi.org/10.1016/j.matdes.2019.107648>.
- [30] N. Kulo et al., *Intermetallics* 114 (2019), <https://doi.org/10.1016/j.intermet.2019.106604>.

- [31] S.K. Kolli et al., *Phys. Rev. Mater.* 4 (11) (2020), <https://doi.org/10.1103/PhysRevMaterials.4.113604> 113604.
- [32] Z.B. Jiao et al., *Prog. Nat. Sci.* 26 (1) (2016) 1, <https://doi.org/10.1016/j.pnsc.2016.01.014>.
- [33] T. Yang et al., *Science* 362 (6417) (2018) 933, <https://doi.org/10.1126/science.aas8815>.
- [34] B. Gludovatz et al., *Science* 345 (6201) (2014) 1153, <https://doi.org/10.1126/science.1254581>.
- [35] J.W. Yeh et al., *Adv. Eng. Mater.* 6 (5) (2004) 299, <https://doi.org/10.1002/adem.200300567>.
- [36] Z. Li et al., *Nature* 534 (7606) (2016) 227, <https://doi.org/10.1038/nature17981>.
- [37] Y. Zhang et al., *Prog. Mater. Sci.* 61 (2014) 1, <https://doi.org/10.1016/j.pmatsci.2013.10.001>.
- [38] T. Yadav et al., *Philos. Mag. Lett.* 97 (12) (2017) 494, <https://doi.org/10.1080/09500839.2017.1418539>.
- [39] N. Zhou et al., *Sci. Bull.* 64 (12) (2019) 856, <https://doi.org/10.1016/j.scib.2019.05.007>.
- [40] S.S. Mishra et al., *J. Mater. Res.* 34 (5) (2019) 807, <https://doi.org/10.1557/jmr.2018.502>.
- [41] S.S. Mishra et al., *J. Alloys Compd.* 832 (2020), <https://doi.org/10.1016/j.jallcom.2020.153764> 153764.
- [42] Z.S. Nong et al., *Trans. Nonferrous Metals Soc. China* 22 (6) (2012) 1437, [https://doi.org/10.1016/S1003-6326\(11\)61338-1](https://doi.org/10.1016/S1003-6326(11)61338-1).
- [43] Y. Meng et al., *Intermetallics* 111 (2019), <https://doi.org/10.1016/j.intermet.2019.106515> 106515.
- [44] G.M. Muralikrishna et al., *Metals* 10 (11) (2020) 1411, <https://doi.org/10.3390/met10111411>.
- [45] C.-H. Chen, Y.-J. Chen, *Scr. Mater.* 162 (2019) 185, <https://doi.org/10.1016/j.scriptamat.2018.11.023>.
- [46] R. Feng et al., *Nat. Commun.* 12 (1) (2021) 1, <https://doi.org/10.1038/s41467-021-23689-6>.
- [47] C. Jiang, B. Gleeson, *Scr. Mater.* 55 (5) (2006) 433, <https://doi.org/10.1016/j.scriptamat.2006.05.016>.
- [48] T. Yang et al., *Scr. Mater.* 164 (2019) 30, <https://doi.org/10.1016/j.scriptamat.2019.01.034>.
- [49] Y.L. Zhao et al., *Acta Mater.* 138 (2017) 72, <https://doi.org/10.1016/j.actamat.2017.07.029>.
- [50] G. Firstov, et al., Electronic and crystal structure of the high entropy TiZrHfCoNiCu intermetallics undergoing martensitic transformation, in: *MATEC Web of Conferences*, EDP Sciences(2015), Vol. 33, p 06006
- [51] A. Chiba et al., *Acta Metall. Mater.* 39 (8) (1991) 1799, [https://doi.org/10.1016/0956-7151\(91\)90148-T](https://doi.org/10.1016/0956-7151(91)90148-T).
- [52] P.A. Bagot et al., *Acta Mater.* 125 (2017) 156, <https://doi.org/10.1016/j.actamat.2016.11.053>.
- [53] T.M. Smith et al., *Nat. Commun.* 7 (1) (2016) 1, <https://doi.org/10.1038/ncomms13434>.
- [54] C.T. Liu, E.P. George, *Scripta Metall. Mater.* 24 (7) (1990) 1285, [https://doi.org/10.1016/0956-716X\(90\)90343-F](https://doi.org/10.1016/0956-716X(90)90343-F).
- [55] E.P. George et al., *Scripta Metall. Mater.* 28 (7) (1993) 857.
- [56] E.P. George et al., *Phys. Status Solidi (A)* 160 (2) (1997) 517, [https://doi.org/10.1002/1521-396X\(199704\)160:2<517::AID-PSSA517>3.0.CO;2-S](https://doi.org/10.1002/1521-396X(199704)160:2<517::AID-PSSA517>3.0.CO;2-S).
- [57] J. Hack et al., *Scr. Metall.* 20 (12) (1986) 1699, [https://doi.org/10.1016/0036-9748\(86\)90272-3](https://doi.org/10.1016/0036-9748(86)90272-3).
- [58] J. Lemaitre, J.-L. Chaboche, *Mechanics of Solid Materials*, Cambridge University Press, 1994.
- [59] P.S. Lobo et al., *Procedia Engineering* 114 (2015) 776, <https://doi.org/10.1016/j.proeng.2015.08.025>.
- [60] K. Otsuka, C.M. Wayman, *Shape memory materials*, Cambridge University Press, 1999.
- [61] T. Omori et al., *Science* 333 (6038) (2011) 68, <https://doi.org/10.1126/science.1202232>.
- [62] K. Otsuka, X. Ren, *Prog. Mater. Sci.* 50 (5) (2005) 511, <https://doi.org/10.1016/j.pmatsci.2004.10.001>.
- [63] J. Xia et al., *Science* 369 (6505) (2020) 855, <https://doi.org/10.1126/science.abc1590>.
- [64] T. Omori et al., *Appl. Phys. Lett.* 101 (23) (2012), <https://doi.org/10.1063/1.4769375> 231907.
- [65] R. Zarnetta et al., *Adv. Funct. Mater.* 20 (12) (2010) 1917, <https://doi.org/10.1002/adfm.200902336>.
- [66] D. Piorunek et al., *Intermetallics* 122 (2020), <https://doi.org/10.1016/j.intermet.2020.106792> 106792.
- [67] C.T. Liu, *Mater. Chem. Phys.* 42 (2) (1995) 77, [https://doi.org/10.1016/0254-0584\(95\)01546-9](https://doi.org/10.1016/0254-0584(95)01546-9).
- [68] O.I. Gorbatov et al., *Phys. Rev. B* 93 (22) (2016), <https://doi.org/10.1103/PhysRevB.93.224106> 224106.
- [69] D.J. Crudden et al., *Acta Mater.* 75 (2014) 356, <https://doi.org/10.1016/j.actamat.2014.04.075>.
- [70] C.T. Liu et al., *Acta Metall.* 33 (2) (1985) 213, [https://doi.org/10.1016/0001-6160\(85\)90139-7](https://doi.org/10.1016/0001-6160(85)90139-7).
- [71] M. Takeyama, C. Liu, Elevated-temperature environmental embrittlement and alloy design of L12 ordered intermetallics, in: *High Temperature Aluminides and Intermetallics*, Elsevier (1992), pp 538.
- [72] C.T. Liu, V.K. Sikka, *JOM* 38 (5) (1986) 19, <https://doi.org/10.1007/BF03257837>.
- [73] C.T. Liu, *Scripta Metall. Mater.* 25 (6) (1991) 1231, [https://doi.org/10.1016/0956-716X\(91\)90392-E](https://doi.org/10.1016/0956-716X(91)90392-E).
- [74] S.C. Deevi, V.K. Sikka, *Intermetallics* 4 (5) (1996) 357, [https://doi.org/10.1016/0966-9795\(95\)00056-9](https://doi.org/10.1016/0966-9795(95)00056-9).
- [75] J. Sato et al., *Science* 312 (5770) (2006) 90, <https://doi.org/10.1126/science.1121738>.
- [76] E.A. Lass et al., *J. Phase Equil. Diffus.* 35 (6) (2014) 711, <https://doi.org/10.1007/s11669-014-0327-5>.
- [77] M. Chen, C.-Y. Wang, *Scr. Mater.* 60 (8) (2009) 659, <https://doi.org/10.1016/j.scriptamat.2008.12.040>.
- [78] M. Hillert, *Acta Mater.* 47 (18) (1999) 4481, [https://doi.org/10.1016/S1359-6454\(99\)00336-5](https://doi.org/10.1016/S1359-6454(99)00336-5).
- [79] Z. Jia et al., *Adv. Mater.* 32 (21) (2020), <https://doi.org/10.1002/adma.202000385> e2000385.
- [80] Z. Sun et al., *Scr. Mater.* 68 (6) (2013) 384, <https://doi.org/10.1016/j.scriptamat.2012.10.040>.
- [81] Z. Ding et al., *Adv. Sustain. Syst.* 4 (5) (2020) 1900105, <https://doi.org/10.1002/adsu.201900105>.
- [82] B. Jiang et al., *Science* 371 (6531) (2021) 830, <https://doi.org/10.1126/science.abe1292>.
- [83] J. Yan et al., *Scr. Mater.* 157 (2018) 129, <https://doi.org/10.1016/j.scriptamat.2018.08.008>.
- [84] R. J. Cava, et al., *Nature* (1994) 367 (6460), 252. [10.1038/367252a0](https://doi.org/10.1038/367252a0).
- [85] J.-K. Bao et al., *Phys. Rev. Mater.* 3 (2) (2019), <https://doi.org/10.1103/PhysRevMaterials.3.024802> 024802.
- [86] Y. Qu et al., *Acta Mater.* 134 (2017) 236, <https://doi.org/10.1016/j.actamat.2017.06.010>.
- [87] T. Watanabe, *J. Mater. Sci.* 46 (12) (2011) 4095, <https://doi.org/10.1007/s10853-011-5393-z>.
- [88] D. Raabe et al., *Curr. Opin. Solid State Mater. Sci.* 18 (4) (2014) 253, <https://doi.org/10.1016/j.cossms.2014.06.002>.
- [89] L. Tan et al., *J. Nucl. Mater.* 441 (1–3) (2013) 661, <https://doi.org/10.1016/j.jnucmat.2013.03.050>.
- [90] S. Curtarolo, et al., *Nat. Mater.* (2013) 12 (3), 191. doi.org/10.1038/nmat3568.
- [91] S. Jiang, K. Yang, *J. Alloys Compd.* (2021), <https://doi.org/10.1016/j.jallcom.2021.158854> 158854.
- [92] F.G. Coury et al., *Sci. Rep.* 8 (1) (2018) 1, <https://doi.org/10.1038/s41598-018-26830-6>.
- [93] X. Fu et al., *Scr. Mater.* 138 (2017) 145, <https://doi.org/10.1016/j.scriptamat.2017.03.014>.
- [94] A.E. Jarfors et al., *Sustainability* 12 (3) (2020) 1059, <https://doi.org/10.3390/su12031059>.
- [95] D. Raabe et al., *Nature* 575 (7781) (2019) 64, <https://doi.org/10.1038/s41586-019-1702-5>.
- [96] J.L. Cann et al., *Prog. Mater. Sci.* 117 (2021), <https://doi.org/10.1016/j.pmatsci.2020.100722> 100722.
- [97] J. Belan, *Mater. Today: Proc.* 3 (4) (2016) 936, <https://doi.org/10.1016/j.matpr.2016.03.024>.
- [98] C. C. Koch, *J. Mater. Sci.* (2007) 42 (5), 1403. doi.org/10.1007/s10853-006-0609-3.
- [99] M.A. Meyers et al., *Prog. Mater. Sci.* 51 (4) (2006) 427, <https://doi.org/10.1016/j.pmatsci.2005.08.003>.
- [100] T. Haubold et al., Nanocrystalline intermetallic compounds—structure and mechanical properties, in: *High Temperature Aluminides and Intermetallics*, Elsevier, 1992, p. 679.
- [101] X.Y. Li et al., *Science* 370 (6518) (2020) 831, <https://doi.org/10.1126/science.abe1267>.
- [102] C.A. Schuh, K. Lu, *MRS Bull.* (2021) 1, <https://doi.org/10.1557/s43577-021-00055-x>.